Temperature-Controlled Behavior of Self-Assembly Gene Delivery Vectors Based on Complexes of DNA with Poly(L-lysine)-*graft*-poly(*N*-isopropylacrylamide)

David Oupický,*,†,‡ Tomáš Reschel,§ Čestmír Koňák,§ and Libuše Oupická‡

Department of Pharmaceutical Sciences, Wayne State University, Detroit, Michigan 48202; CRC Institute for Cancer Studies, University of Birmingham, Birmingham, UK; and Institute of Macromolecular Chemistry, Academy of Sciences of the Czech Republic, Prague

Received January 13, 2003; Revised Manuscript Received July 2, 2003

ABSTRACT: Synthetic gene delivery vectors based on polyelectrolyte complexes of nucleic acids and polycations are widely studied as safe substitutes of viral vectors. Here, we synthesized a series of thermoresponsive graft copolymers (TRC) of poly(L-lysine) (PLL) and poly(*N*-isopropylacrylamide) (PNIPAM) and evaluated temperature-responsive properties of their polyelectrolyte complexes with plasmid DNA using a range of light scattering techniques. The PNIPAM-containing complexes, swollen bellow the phase transition temperature of PNIPAM grafts, exhibited a significant increase in structural density when the temperature increased above the phase transition. The changes in the structural density of the DNA complexes increased with increasing PNIPAM content and were almost independent of PNIPAM molecular weight. The expected corresponding reduction of sizes of the complexes upon increasing the temperature above the PNIPAM phase transition was observed for complexes of TRC with the highest PNIPAM content and for complexes formed at lower molar mixing ratios. In addition, the surface charge of the complexes was also modulated by temperature. The absolute values of the surface charge (ζ potential) increased as the PNIPAM grafts collapsed above their phase transition temperature. The presence of PNIPAM in the complexes resulted in a higher susceptibility toward polyelectrolyte exchange reactions with heparin when compared with parent PLL. In addition, the ability of heparin to liberate DNA from the complexes declined with increasing the time between the formation of the complexes and the addition of heparin. A time-dependent conversion of the supercoiled form of plasmid DNA into the relaxed form when present in the polyelectrolyte complexes was also observed.

Introduction

The availability of efficient and safe means of in vivo delivery of genes is a crucial requirement for a successful introduction of human gene therapy. Delivery methods employing synthetic nonviral self-assembly vectors based on polyelectrolyte complexes of DNA with cationic polymers are being extensively studied as safe alternatives to genetically modified viruses. Despite vast progress in the development of the nonviral vectors in recent years, significant constraints limiting the efficiency of the delivery process still remain. The typical low transfection activity after systemic administration is to a great extent caused by the inability of the nonviral vectors to overcome the multitude of barriers encountered between the site of administration and localization in the cell nucleus of the target tissue.[1−3]

The major barriers to efficient nonviral gene delivery fall into two categories. The first include barriers encountered during the extracellular phase of the delivery process, while the second include barriers faced by the vectors inside the target cells. The existing evidence suggests that many of these complications ultimately relate to biophysical characteristics of the vectors such as surface properties, size, and affinity of the polycation to DNA that determine their behavior. The barriers faced by the vectors often demand greatly different biophysical and biological properties. Consequently, such vectors are unlikely to rely on a single molecule capable of overcoming all the encountered barriers. The vectors of the future are likely to adopt more sophisticated strategies to efficiently deliver and control gene activity in vivo. One of the major challenges is to find an approach that would integrate the contradictory functional features necessary to allow efficient gene delivery within a single vector—a vector that would be biologically inert and physically stable during extracellular phase of the delivery, yet capable of a programmed disassembly and translocation to a cell nucleus after arrival at the target tissue. In many aspects similar to natural viruses, such a vector has to be able to recognize changes in the environment and to respond actively to them by changing its properties or behavior.[4] For example, vectors capable of changing their properties in response to redox potential and pH gradients found between extracellular space and some intracellular compartments have been investigated in various sophisticated gene delivery strategies.[5−12] The intracellular pH gradients have also been exploited when using polycations with inherent buffering capacity in the endosomal pH range to construct some of the most efficient gene delivery vectors.[13−15]

An emerging group of stimulus-responsive gene delivery vectors relies on polymers capable to undergo phase transition in response to changes in the environment. To date, only polycations capable of responding to changes in temperature were investigated in this group.[16−19] This approach is, despite the limited progress so far, very promising not only due to fast, highly nonlinear, and reversible nature of the responses to

† Wayne State University.
‡ University of Birmingham.
§ Academy of Sciences of the Czech Republic.
* Corresponding author: tel 313-993-7669; fax 313-577-2033; e-mail oupicky@wayne.edu.

10.1021/ma034039a CCC: $25.00
Published on Web 08/01/2003

small changes in the environment but also due to the number of possible stimuli that can be exploited.[20,21] Temperature-responsive vectors described thus far use copolymers of *N*-isopropylacrylamide (NIPAM) as the temperature-responsive component. Poly(*N*-isopropylacrylamide) (PNIPAM) represents probably the most often-used thermoresponsive polymer in biotechnology and medicine because of its phase transition temperature at 32 °C.[22,23] Copolymers of *N*-isopropylacrylamide, 2-(dimethylamino)ethyl methacrylate, and butyl methacrylate were synthesized and studied as temperature-responsive gene delivery vectors.[18] The use of a copolymer with the phase transition 21 °C enabled controlling the affinity of the copolymer to plasmid DNA. While the DNA was fully retained in the origin of the gel during electrophoresis at temperatures above the phase transition, at temperatures below the phase transition the plasmid became partially dissociated from the copolymer. In addition, the authors established that a temperature regime can be found that enables to control the disassembly of the vector inside the cells and achieve elevated transfection levels.[18]

This study proposes a design for novel temperature-responsive DNA delivery vectors based on graft copolymers of poly-L-lysine and PNIPAM and reports results obtained from the initial studies of their temperature-dependent properties. The key motivation for the development and study of such vectors is the requirement for diverse properties necessary to overcome the barriers encountered by the vectors during gene delivery. We believe that the complexes described in this study have the potential to form a design platform for future development of first truly artificial viruses and their practical application in gene therapy.

Experimental Section

Two poly(L-lysine) hydrobromides (PLL) with $M_w = 87.6 \times 10^3$ ($M_w/M_n = 1.29$) and $M_w = 19.6 \times 10^3$ ($M_w/M_n = 1.3$) and porcine heparin sodium salt were obtained from Sigma. *N*-Isopropylacrylamide and 2,2′-azobis(isobutyronitrile) (AIBN) were purchased from Aldrich. A circular 5.2 kb plasmid vector pGL3-control was from Promega and SYBR Gold from Molecular Probes.

Synthesis and Analysis of Polymers. The synthesis of the copolymers used in this study was described previously by Konak et al.[24] Briefly, semitelechelic poly(*N*-isopropylacrylamide) with a terminal carboxyl group was prepared by radical polymerization of NIPAM (1.19 mol/L) in the presence of 3-mercaptopropionic acid (MPA) (24.4 or 65.9 mmol/L) as a chain transfer agent. Weight- and number-average molecular weights (M_w and M_n) of semitelechelic PNIPAM were determined by size exclusion chromatography using the ÄKTA explorer system (Amersham Pharmacia Biotech.) equipped with a refractive index and multiangle light scattering detector DAWN DSP-F (Wyatt Technology Corp., Santa Barbara, CA) using a TSK 4000SW column (BECKMAN Instruments) in 80% methanol and 20% 0.3 M sodium acetate (pH 6.5). The content of the end carboxylic groups of semitelechelic PNIPAM was determined by potentiometric titration with NaOH and used to calculate the number-average molecular weight ($M_{n,T}$) assuming one carboxyl end group per macromolecule. The PNIPAM synthesized using 65.9 mmol/L MPA had $M_n = 4.6 \times 10^3$, $M_w/M_n = 3.5$, and $M_{n,T} = 4.2 \times 10^3$; the PNIPAM synthesized using 24.4 mmol/L MPA had $M_n = 17.6 \times 10^3$, $M_w/M_n = 1.9$, and $M_{n,T} = 12.4 \times 10^3$.

Graft copolymers PLL-*g*-PNIPAM were synthesized by reacting freshly prepared succinimidyl esters of the two PNIPAM polymers with PLL ($M_w = 87.6 \times 10^3$) aiming to prepare copolymers containing 25, 50, and 75 wt % of PLL. The reactions were carried out for 48 h in dry dimethyl sulfoxide in the presence of triethylamine at 20 °C. The polymers were isolated by precipitation into excess of diethyl ether and purified by acetone extraction and extensive dialysis against water (membrane with molecular weight cutoff 5×10^4). The content of PLL in the graft copolymers was determined by ^{1}H NMR analysis from the values of integral intensity of selected PLL and PNIPAM proton peaks (Table 1). The thermoresponsive graft copolymers are abbreviated as TRC(*x*,*y*), where *x* is molecular weight ($M_{n,T} \times 10^{-3}$) of PNIPAM grafts and *y* is weight content (wt %) of PNIPAM in the copolymer.

Table 1. Molecular Characteristics of Thermoresponsive Graft Copolymers

copolymer	PNIPAM content (wt %)	$M_{n,T}$ of PNIPAM grafts	M_w of copolymer	grafting density (mol %)	d*n*/d*c*
TRC(4.2, 62)	62	4 200	230 000	7.9	0.178
TRC(4.2, 42)	42	4 200	150 000	3.5	0.181
TRC(4.2, 21)	21	4 200	110 000	1.3	0.185
TRC(12.4, 55)	55	12 400	190 000	2.0	0.179
TRC(12.4, 42)	42	12 400	150 000	1.6	0.181
TRC(12.4, 21)	21	12 400	110 000	0.8	0.185

Formulation of Polyelectrolyte DNA Complexes. Polycation/DNA complexes were prepared at pH = 7.4 in water or HEPES buffer at desired molar mixing ratio φ ($\varphi = c$(PLL amines)/c(DNA phosphates)) by mixing equal volumes of a polycation and plasmid DNA (40 μg/mL). Mass of 325 per one phosphate group was used in the calculations.

Static Light Scattering. The static light scattering was measured with purpose build goniometer in vertically polarized light at wavelength 632.8 nm, angular range 30−140°, and temperatures 25 and 38 °C. On every temperature change, the measurements were realized after reaching steady-state conditions (typically after 20 min). The apparatus was calibrated with benzene at a 90° scattering angle. The static light scattering data were analyzed by the Zimm plot to obtain apparent molecular weights $M_w = R(0,c)/Kc$ of the DNA complexes, assuming the compositional heterogeneity of the complexes was negligible (K is the optical constant which includes the square of the refractive index increment d*n*/d*c*; $R(\theta)$ is the Rayleigh ratio, proportional to the intensity of the light scattered from solutions and the complex concentration c in g/mL). Extrapolation to zero scattering angle was carried out by linear or quadratic fits of the scattering curves. Extrapolation to zero concentration was not performed due to very low concentrations of the complexes ($\sim 10^{-5}$ g/mL). An improved algorithm of data analysis based on a model of solid spheres in the Rayleigh approximation was used for more aggregated systems.[25,26] The accuracy of the measurements was better than 3%.

The refractive index increments, d*n*/d*c*, of the copolymers were calculated as weight-average values of the individual components. The refractive index increment for PNIPAM, 0.190 in water, was measured with a Brice-Phoenix refractometer at the light wavelength of 633 nm, and the value of 0.188 for PLL was taken from literature. The calculated d*n*/d*c* values are collected in Table 1. They were used for analyses of light scattering data at both temperatures (25 and 38 °C), assuming that the temperature effect is small.[27] Calculation of concentrations and refractive index increments of the complexes as a function of the molar mixing ratios was carried out using the previously published model of complex formation.[28]

Dynamic Light Scattering. Polarized DLS measurements were made at five angles in the angular range 30−120° using a light scattering apparatus equipped with a He−Ne (632.8 nm) and ALV 5000, multibit, multitau autocorrelator covering approximately 10 decades in delay time τ. The inverse Laplace transformation using the REPES method of constrained regularization was used for analysis of time autocorrelation functions. REPES directly minimizes the sum of the squared differences between the experimental and calculated intensity−time correlation functions using nonlinear programming. This method uses an equidistant logarithmic grid with fixed

components (here a grid of 10 components per decade) and determines their amplitudes. As a result, a scattered light intensity distribution function $A(\tau)$ of decay times is obtained, which can be easily transformed into a distribution function of hydrodynamic sizes.

The time autocorrelation functions were also fitted assuming the Pearson distribution of characteristic relaxation times, τ_c:

$$z(\tau_c) = \tau_o^{\,p}\, \tau_c^{\,-p-1} \exp(-\tau_o/\tau_c)/\Gamma(p)$$

where τ_o and p are parameters and $\Gamma(p)$ is the Gamma function of parameter p. The Pearson distribution was chosen for the simplicity of its mathematical treatment. The average apparent hydrodynamic radius, R_H, was calculated from the zero angle limit of the apparent diffusion coefficient obtained mostly by linear extrapolation using the Stokes−Einstein equation:

$$R_H = kT/6\pi\eta D$$

where k is the Boltzmann constant, T is the absolute temperature, and η is the viscosity of water. The experimental error of R_H determination for the complexes was typically about 3%.

The apparent structural density (ρ) of DNA complexes was calculated as an equivalent average density from M_w for the model of a sphere with the radius R_H with no correction for polydispersity ($\rho = 3M_w/4\pi N_A R_H^3$). The statistical significance of the observed temperature-induced changes of structural density of TRC-based complexes was confirmed by paired Student's t-test ($P < 0.01$).

Electrophoretic Light Scattering. Measurements of the zeta (ζ) potential were made using a Zetasizer 3000HS (Malvern Instruments, UK) fitted with a 50 mW Uniphase green laser operating at a wavelength of 532 nm. Measurements of all samples were carried out at 25 and 38 °C. The samples, prepared in 1 mM HEPES buffer pH 7.4, were left in the instrument for 45 min at the required temperature for equilibration to occur prior to measurements being taken. At least 10 measurements were made of each sample to check for repeatability. The measured electrophoretic mobilities (μm/cm/V/s) were converted to ζ potential (mV) using the Smoluchowski approximation. A reference measurement using the Malvern ζ potential standard was run prior to each sample analysis to check for correct instrument operation. The statistical significance of the observed temperature-induced changes of ζ potentials in TRC-containing complexes was confirmed by paired Student's t-test ($P < 0.01$).

Dye Exclusion Assay. The ability of the copolymers to condense DNA was evaluated by dye exclusion assay using SYBR-Gold dye. The complexes were prepared using plasmid DNA solution containing 5x SYBR-Gold using molar mixing ratios φ in the interval 0−3. 200 μL of each sample was then transferred into a black polystyrene 96-well-flat-bottom assay plate, and the fluorescence intensity of all samples was measured at once using Wallac Victor^2 1420 multilabel counter (Perkin-Elmer, UK) using excitation λ_{exc} = 485 nm and emission λ_{em} = 535 nm filters and counting time 1 s. The fluorescence intensities were measured first at 25 °C and then at 38 °C, allowing 45 min for temperature equilibration. The condensation curves (relative fluorescence intensity vs φ) at both 25 and 38 °C were constructed using appropriate fluorescence intensity of DNA/SYBR-Gold(5x) as 100% and that of SYBR-Gold(5x) as 0%. The experiment was repeated on two separate occasions—the relative data differing by less than 5%.

Gel Retardation Assay. To assay the ability of copolymers to retard movement of plasmid DNA in the agarose gel, the complexes of DNA with the copolymers were formed as described above using the range of $\varphi = 0-2$. The samples were then loaded on to a 0.8% agarose gel containing 0.5 μg/mL ethidium bromide and run for 1 h at 120 V in 0.5x TBE buffer. The gels were then scanned by a Typhoon gel scanner (Pharmacia, UK) set at 533 nm/610 nm wavelengths and 50 μm resolution.

Polyelectrolyte Exchange Reactions. Polyelectrolyte exchange reactions were studied by observing heparin-mediated release of free DNA from the complexes with TRC(4.2, 62), PLL ($M_w = 87.6 \times 10^3$), and PLL ($M_w = 19.6 \times 10^3$) by agarose gel electrophoresis. Complexes of plasmid DNA with TRC(4.2, 62) and PLL ($M_w = 87.6 \times 10^3$) were prepared as described above at $\varphi = 1.2$ and 2. The complexes were prepared either "fresh" 1 h before or 24 h before heparin addition. The complexes were therefore incubated either for 1 h at 25 °C or for 24 h at 25 or 37 °C before 10 μL of heparin (6 mg/mL solution in 1 mM EDTA containing 250 mM phosphate/TRIS buffer pH 8.5) was mixed with 10 μL of complexes and left to incubate for an additional 2 h at 25 °C. The mixture was then applied on the 0.8% agarose gel containing 0.5 μg/mL ethidium bromide and run for 60 min at 120 V in 0.5x TBE buffer (pH = 8.5). Appropriate DNA controls treated in the same way as the complexes were included in the gels. Complexes of DNA with PLL ($M_w = 19.6 \times 10^3$) formed at $\varphi = 2$ were prepared 0.5−1−2.5−5−24 h before addition of heparin and analyzed by agarose gel electrophoresis as described above. A Typhoon gel scanner (Pharmacia, UK) set at 533 nm/610 nm wavelengths and 50 μm resolution was used to scan the gel. The total quantities of released DNA as well as the proportions of supercoiled and relaxed form in the released DNA were analyzed using ImageQuant software.

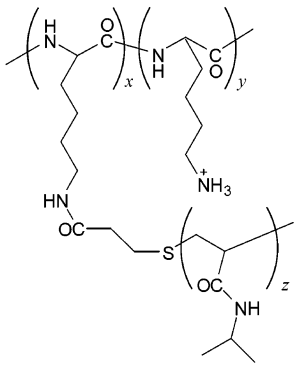

Figure 1. Structure of thermoresponsive PLL-*g*-PNIPAM copolymers.

Effect of Temperature on the Morphology of TRC/DNA Complexes Using Transmission Electron Microscopy. TRC(4.2/62)/DNA complexes were prepared as described above at $\varphi = 1.2$ and 2. 5 μL of the solution was dispensed onto 200 mesh carbon-coated copper grids at 25 or 37 °C and left for several hours to dry. The mesh was washed in deionized water, and complexes were stained with uranyl acetate (10 μL of 2% freshly filtered solution) for 2 min. The staining solution was carefully removed by filter paper, and the mesh was washed by immersion in water and left to dry. The whole preparation procedure of the samples above the phase transition of PNIPAM was carried out in a hot room with temperature maintained at 37 °C. This guaranteed that all the manipulations with the DNA complexes, all the solutions, and all the surfaces that came into a contact with the complexes were maintained above the phase transition temperature. The samples were left in the hot room until the mesh was fully dried. The samples were then viewed using a Joel 1200 EX transmission electron microscope.

Results and Discussion

Thermoresponsive graft copolymers (Figure 1) were synthesized by randomly grafting succinimidyl ester of semitelechelic PNIPAM onto PLL ($M_w = 87.6 \times 10^3$). The semitelechelic PNIPAM precursors were prepared by radical solution polymerization as described previously.[24] The molecular weights of the PNIPAM precursors were determined by end group titration and size exclusion chromatography. Good agreement between the M_n and $M_{n,T}$ values was observed for PNIPAM with lower molecular weight. A larger difference was observed for the PNIPAM with higher molecular weight,

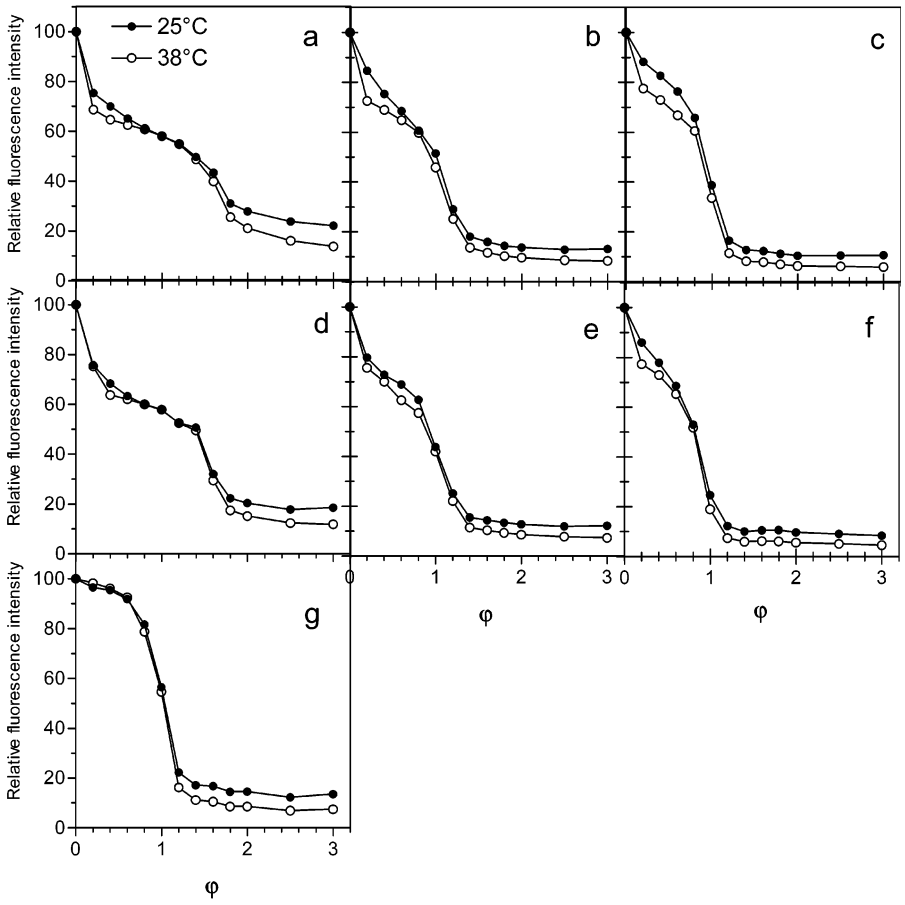

Figure 2. Fluorescent dye exclusion assay. The ability of TRC and PLL to condense DNA was evaluated by the dye exclusion assay using SYBR-Gold dye. The complexes were prepared using plasmid DNA solution containing SYBR-Gold using molar mixing ratios $\varphi = 0-3$. Fluorescence intensity of all samples was measured using excitation $\lambda_{exc} = 485$ nm and emission $\lambda_{em} = 535$ nm first at 25 °C (●) and then at 38 °C (○), allowing 45 min for temperature equilibration. The complexes were formed using the following copolymers (TRC(*x*, *y*), where *x* is the molecular weight ($M_{n,T} \times 10^{-3}$) of PNIPAM grafts and *y* is the weight content (wt %) of PNIPAM in the copolymer): TRC(4.2, 62) (a), TRC(4.2, 42) (b), TRC(4.2, 21) (c), TRC(12.4, 55) (d), TRC(12.4, 42) (e), TRC-(12.4, 21) (f), and PLL (g).

indicating the possible presence of bifunctional molecules in the sample. Notorious difficulties with chromatographic determinations of molecular weights of PNIPAM polymers together with decreased precision of the end group titration for the copolymer with higher molecular weight could additionally contribute to the observed differences. PNIPAMs with molecular weights 4.2×10^3 and 12.4×10^3 were prepared and used to synthesize two series of graft copolymers with PLL; TRC(4.2, *y*) and TRC(12.4, *y*) varying in PNIPAM content (Table 1). The synthesized TRC allowed evaluation of both the effects of PNIPAM content and PNIPAM molecular weight on the physicochemical properties of the polyelectrolyte complexes of TRC with plasmid DNA. Since the copolymers with different PNIPAM molecular weights were prepared to contain similar weight fractions of PNIPAM, differential grafting density needs to be considered as an additional factor influencing the condensation ability and other properties of TRC (Table 1).

The dye exclusion assay that was used to monitor DNA condensation relies on following changes in fluorescence intensity of SYBR Gold while increasing molar mixing ratios φ (Figure 2). SYBR Gold is an unsymmetrical cyanine dye that exhibits more than a 1000-fold fluorescence enhancement upon binding to nucleic acids. As a polycation interacts with DNA, it replaces the dye and fluorescence intensity decreases. DNA condensation curve for PLL shows a typical sigmoidal profile with the main transition around point of charge equivalency ($\varphi \sim 1$) (Figure 2g). Although all the synthesized TRC were able to condense DNA (Figure 2a−f), increasing content of PNIPAM resulted in systematic changes of the condensation profiles observed in both TRC series. The shapes of the condensation curves changed with increasing the PNIPAM content in the TRC from that observed for PLL (an abrupt drop in the fluorescence intensity) to curves with a more gradual decrease of fluorescence intensity. The condensation curves for TRC with the highest PNIPAM content also displayed a clear shift of the main transition to higher φ and appearance of a second transition at $\varphi < 0.2$ (Figure 2a,d).

All the properties of TRC/DNA complexes in this study were evaluated at two temperatures: below (at 25 °C) and above (at 38 °C) PNIPAM phase transition temperature. The fluorescence intensity of SYBR Gold containing complexes prepared in the range of $\varphi = 0-3$ was measured first at 25 °C and then after 30 min equilibration at 38 °C measured again. The data in Figure 2 show that the temperature increase did not affect the horizontal position of the condensation curves, i.e., φ where the main transitions were observed. However, earlier decrease of relative fluorescence intensity in the initial phases of the condensation ($\varphi < 1$) in the case of PNIPAM containing copolymers could be

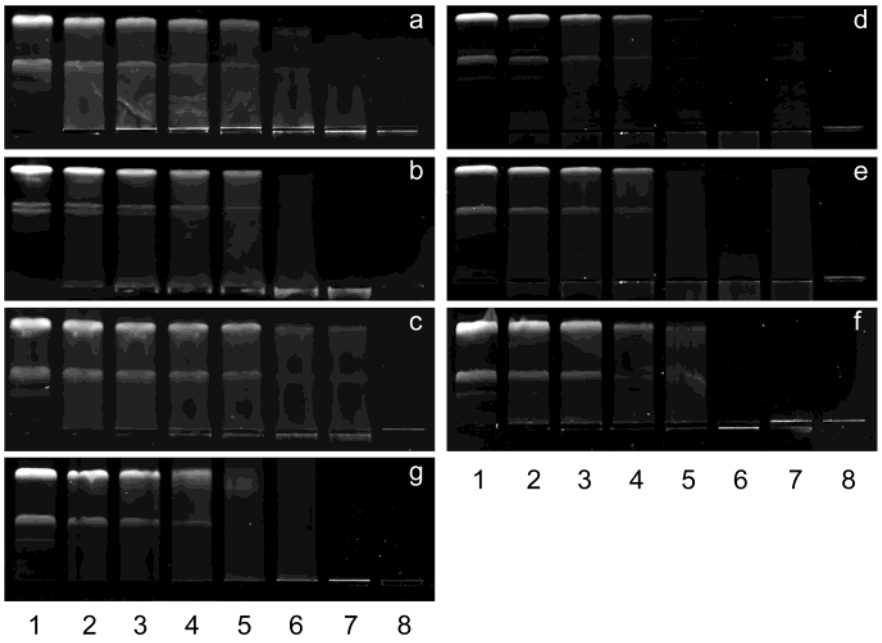

Figure 3. Gel retardation assay. TRC/DNA and PLL/DNA complexes were formed at varying φ and analyzed on 0.8% agarose gel containing 0.5 μg/mL ethidium bromide. In each case, gels present complexes formed at $\varphi = 0$ (lane 1), 0.2 (lane 2), 0.4 (lane 3), 0.6 (lane 4), 0.8 (lane 5), 1.0 (lane 6), 1.2 (lane 7), and 2.0 (lane 8). The complexes were formed using using the following copolymers (TRC(x, y), where x is the molecular weight ($M_{n,T} \times 10^{-3}$) of PNIPAM grafts and y is the weight content (wt %) of PNIPAM in the copolymer): TRC(4.2, 62) (a), TRC(4.2, 42) (b), TRC(4.2, 21) (c), TRC(12.4, 55) (d), TRC(12.4, 42) (e), TRC(12.4, 21) (f), and PLL (g).

observed. In addition, decreased residual fluorescence intensities were observed for all samples. Typically, lower residual fluorescence intensities suggest more efficient displacement of the fluorescent dye from DNA, indicating a formation of more tightly packed complexes above the phase transition temperature. Figure 2 confirms that the condensation properties of TRC are predominantly governed by PNIPAM content, whereas the molecular weight of PNIPAM grafts does not have a significant effect.

A gel retardation assay was used in parallel with the dye exclusion assay to monitor formation of the TRC/DNA complexes. This assay allows to monitor migration pattern of DNA in agarose gel and can therefore provide additional insights into the mechanism of condensation of nucleic acids.[29] To verify efficient DNA condensation by TRC, complexes were prepared in the range of $\varphi = 0-2$ and analyzed on 0.8% agarose gel (Figure 3). Corresponding to the dye exclusion assay, PLL demonstrated the most efficient condensation ability, with DNA being fully retained in the loading well at $\varphi > 0.8$ (Figure 3g). Despite some differences, all TRC showed very similar behavior to PLL with full DNA retardation generally observed at $\varphi \geq 1.0$. Nevertheless, as demonstrated on the example of TRC(4.2, 62)/DNA complexes (Figure 3a), higher fluorescence intensity was observed in the gel both in the loading well and in the gel, confirming results of the dye exclusion assay (even though ethidium bromide was used to stain the gels instead of SYBR Gold used in the dye exclusion). Nevertheless, despite apparently somewhat reduced ability of TRC with the highest PNIPAM content to displace fluorescent dye from DNA, no free DNA was observed in the gel at $\varphi \geq 1.0$.

To restrict the experimental work, we carried out further studies with complexes prepared at two molar mixing ratios. The graft copolymers used in this study associate above their phase transition temperature into particles with radius 40−200 nm.[30] To minimize the effect of free TRC on the obtained data, we chose to study complexes prepared at $\varphi = 1.2$. Only a small amount of free TRC can be expected present at this molar mixing ratio, yet none of the studied complexes showed any free DNA at this composition. On the other hand, results in Figures 2 and 3 suggested less efficient condensation in the case of TRC with the highest PNIPAM content. For that reason, we have selected a second molar mixing ratio $\varphi = 2$ at which better DNA condensation was achieved.

Several physicochemical parameters were identified to affect performance of polyelectrolyte complexes as gene delivery vectors. For example, the size of the complexes affects both intra- and extracellular trafficking; surface characteristics like hydrophobicity and charge play a significant role in interactions with immune system and during cellular uptake. Since this study represents the first evaluation of these graft copolymers as gene delivery vectors, we have employed a range of light scattering techniques to obtain information on the temperature-dependent behavior of the TRC/DNA complexes. We routinely measured the following three basic molecular parameters for each TRC/DNA formulation: (1) hydrodynamic radius (R_H), (2) ζ potential, and (3) molar mass (M_w). We also calculated structural density (ρ) of the prepared complexes using M_w and R_H.

Data summarizing the dependence of the three major studied parameters (R_H, ζ, ρ) on PNIPAM content and their changes upon increasing the temperature from 25 to 38 °C are shown for TRC/DNA complexes prepared at $\varphi = 1.2$ using both series of copolymers TRC(4.2, y) and TRC(12.4, y) in Figures 4 and 5. Zimm plots for the TRC(4.2, y)/DNA complexes are shown for illustration of the quality of the static light scattering measurements (Figure 4d). The size of the complexes showed a clear tendency to increase with increasing PNIPAM

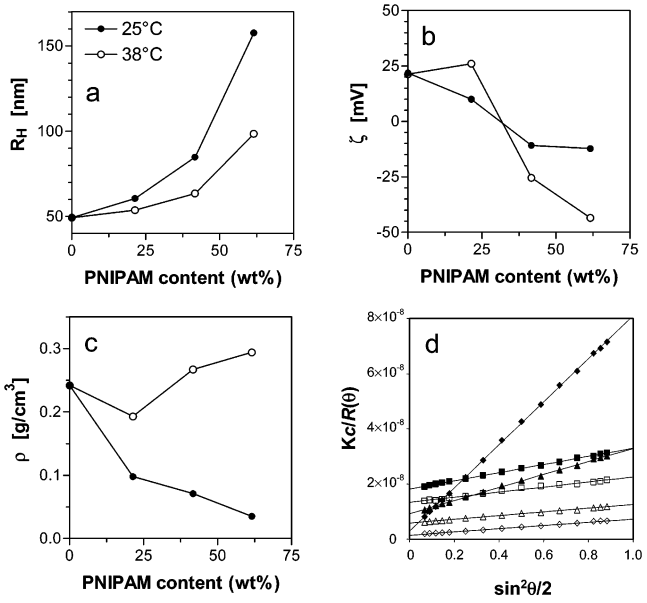

Figure 4. Effect of temperature on molecular parameters of TRC(4.2, *y*)/DNA complexes formed at $\varphi = 1.2$. The DNA complexes were formed using TRC copolymers containing PNIPAM with molecular weight 4200, and (a) hydrodynamic radius (R_H), (b) ζ-potential, and (c) structural density (ρ) of the TRC(4.2, *y*)/DNA complexes were determined at 25 °C (●) and 38 °C (○). A Zimm plot of scattering curves at 25 °C (full symbols) and 38 °C (open symbols) is shown in (d): TRC(4.2, 62) (diamonds), TRC(4.2, 42) (triangles), TRC(4.2, 21) (squares).

contents at 25 °C. The increase was particularly apparent in formulations with >50% PNIPAM in the used copolymers. The structural density of the TRC/DNA complexes decreased with increasing content of PNIPAM in the copolymers, indicating an internal swelling of the complexes by hydrated PNIPAM chains. Similar trends in size and structural density were observed for DNA complexes of graft copolymers that contained poly[*N*-(2-hydroxypropyl)methacrylamide] instead of PNIPAM as the hydrophilic nonionic block.[31] Interestingly, the PNIPAM-containing complexes showed a high degree of aggregation (number of DNA molecules per 1 complex) at $\varphi = 1.2$. The aggregation levels increased with increasing PNIPAM content, and they were somewhat lower for PNIPAM(12.4)-based complexes. The ζ potential of the complexes decreased with increasing PNIPAM content from positive values observed for PLL/DNA complexes to negative values observed for TRC/DNA complexes with PNIPAM content above 25%.

Increasing temperature above the phase transition of PNIPAM caused noticeable changes in most of the observed parameters. As expected, the temperature-induced changes were more clearly manifested in samples with higher content of the thermoresponsive component (Figures 4 and 5). The sizes of the complexes decreased as a consequence of the collapse of PNIPAM chains within the complexes. This was also accompanied by a marked increase in the structural density (8.5 times for TRC(4.2, 62)/DNA complexes), reaching even higher values than those observed for PLL/DNA complexes. The temperature-induced rise of the structural density was more evident in complexes with higher PNIPAM contents. A small, temperature-induced aggregation was observed when the temperature was increased to 38 °C. The molecular weight of the complexes increased in a PNIPAM-dependent fashion by a factor of 1.2−2.1. The increase of temperature affected also ζ potential of the

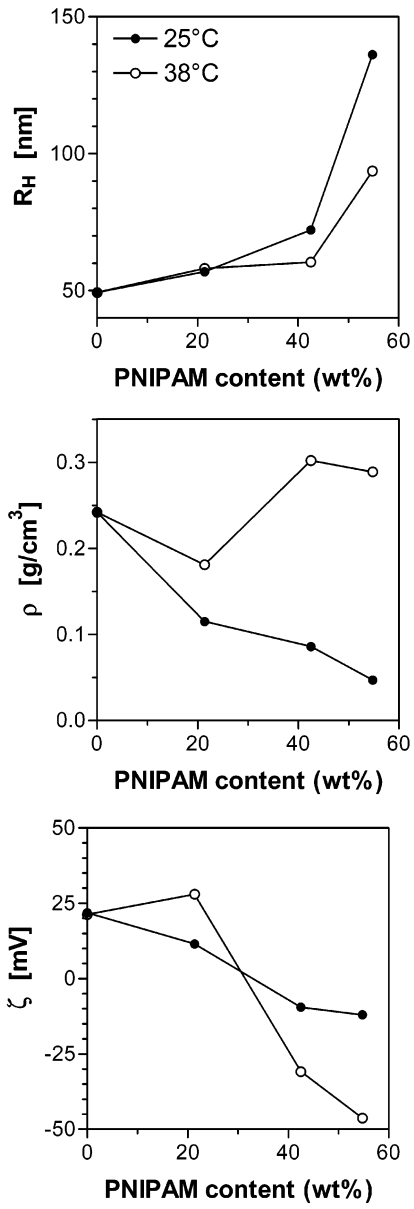

Figure 5. Effect of temperature on molecular parameters of TRC(12.4, *y*)/DNA complexes formed at $\varphi = 1.2$. The DNA complexes were formed using TRC copolymers containing PNIPAM with molecular weight 12 400, and hydrodynamic radius (R_H), structural density (ρ), and ζ-potential of the TRC-(12.4, *y*)/DNA complexes were determined at 25 °C (●) and 38 °C (○).

PNIPAM-containing complexes. Absolute ζ potential values increased, probably as the masking effect of PNIPAM molecules was reduced after their collapse above the phase transition temperature. Control PLL/DNA complexes, on the other hand, showed only negligible temperature-induced changes.

The negative ζ potential values together with the dye exclusion and gel retardation results suggested insufficient condensation ability of the TRC with the highest PNIPAM contents at $\varphi = 1.2$. Two reasons can possibly explain this reduced condensation ability (i) a systematic error in quantification of the amino groups in the TRC, caused by the presence of PNIPAM, and (ii) the heterogeneity of the TRC that may contain macromolecules with a very high content of PNIPAM, preventing DNA condensation and therefore effectively decreasing the concentration of amino groups available for condensation.

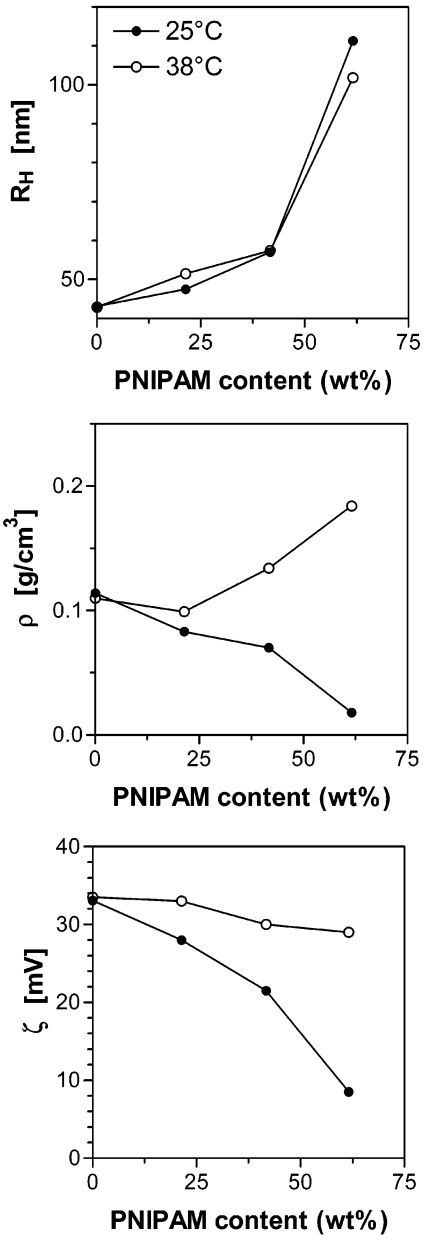

Figure 6. Effect of temperature on molecular parameters of TRC(4.2, *y*)/DNA complexes formed at $\varphi = 2$. The DNA complexes were formed using TRC copolymers containing PNIPAM with molecular weight 4200, and hydrodynamic radius (R_H), structural density (ρ), and ζ-potential of the TRC-(4.2, *y*)/DNA complexes were determined at 25 °C (●) and 38 °C (○).

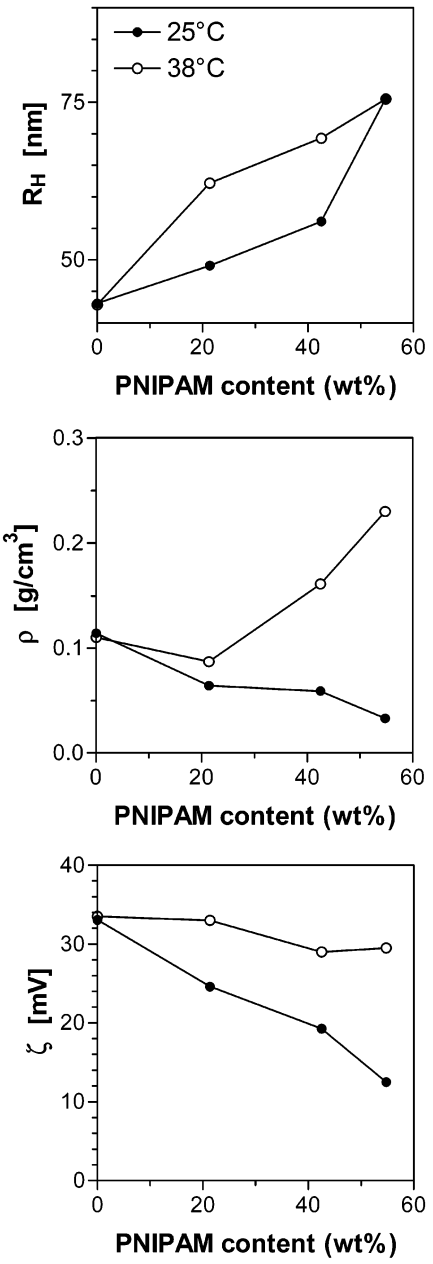

Figure 7. Effect of temperature on molecular parameters of TRC(12.4, *y*)/DNA complexes formed at $\varphi = 2$. The DNA complexes were formed using TRC copolymers containing PNIPAM with molecular weight 12 400, and hydrodynamic radius (R_H), structural density (ρ), and ζ-potential of the TRC-(12.4, *y*)/DNA complexes were determined at 25 °C (●) and 38 °C (○).

The general trends in the behavior observed for the complexes formed at $\varphi = 1.2$ were observed also for the complexes formed at $\varphi = 2.0$ (Figures 6 and 7). The increase in sizes of the complexes with increasing PNIPAM content at 25 °C was apparent even at low PNIPAM contents, mainly because of greatly reduced aggregation compared to the complexes formed at $\varphi = 1.2$. Formation of nearly mono-DNA-containing complexes was observed. The internal swelling of the TRC/DNA complexes by PNIPAM chains below their phase transition was verified also for complexes formed at $\varphi = 2$ as the structural density decreased with increasing PNIPAM content. In general, the complexes formed at $\varphi = 2$ were smaller and had lower structural density than corresponding complexes formed at $\varphi = 1.2$. The improved condensation ability of the TRC with high PNIPAM contents at $\varphi = 2$ was demonstrated by positive values of ζ potentials for all the studied complexes. The screening effect of PNIPAM on the surface charge, similar to that observed for other hydrophilic polymers (i.e., poly(ethylene glycol)), was confirmed by the decrease of ζ potential with increasing PNIPAM content.

The structural parameters of the TRC/DNA complexes prepared at $\varphi = 2$ did not undergo as apparent changes as those of the complexes formed at $\varphi = 1.2$. The sizes of TRC(4.2, *y*)/DNA complexes exhibited only negligible variations upon raising the temperature from 25 to 38 °C (Figure 6), whereas mixed results with significant increases of sizes for some complexes were observed for TRC(12.4, *y*)/DNA series of complexes

(Figure 7). The structural density, on the other hand, increased with increasing PNIPAM content as the temperature was raised above the PNIPAM phase transition. The values of structural density increased by similar factors as in the case of complexes prepared at $\varphi = 1.2$ (10.2-fold for TRC(4.2, 62)/DNA). The absolute values of ζ potentials increased to highly positive values after raising the temperature to 38 °C (Figures 6 and 7).

When comparing the effects of increasing temperature on the sizes of the complexes prepared at $\varphi = 2$ with complexes prepared at $\varphi = 1.2$, one needs to take into account greater temperature-induced aggregation observed for the complexes formed at $\varphi = 2$. For instance, only about 2-fold increase of M_w was observed for TRC(4.2, 62)/DNA complexes when formed at $\varphi = 1.2$, whereas an almost 8-fold increase was found when they were prepared at $\varphi = 2$. This clear difference can probably be attributed to the effect of free copolymers (especially those with high PNIPAM contents) on the aggregation of the complexes, at least partly due to their association with the complexes above the PNIPAM phase transition. The association through the collapsed hydrophobic PNIPAM domains in the complexes and in the free copolymers is, apart from the aggregation of the complexes, the most likely additional mechanism of the molecular weight increase.

Polyelectrolyte complexes formed in water often exhibit a high degree of aggregation, and the presence of low concentrations of salts during complex formation can lead to much lower aggregation levels.[32] In this study, we have prepared the polyelectrolyte complexes in water (pH of the complexes always adjusted to 7.4) despite the pseudo-irreversible character of such complexes.[33,34] The reduced degree of temperature-induced aggregation of the complexes formed in water enabled us to better study the temperature responsiveness of the complexes. The presence of salts resulted in excessive aggregation at 38 °C as illustrated in Figure 8. The figure shows the effect of the presence of 10 mM HEPES buffer on hydrodynamic radii and structural density of TRC(12.4, *y*)/DNA complexes formed at $\varphi = 1.2$. Guinier plots of scattering curves of the TRC(12.4, *y*)/DNA complexes measured at 38 °C are shown in Figure 8c. Unlike the results obtained in water, raising the temperature increased the sizes of the complexes. The aggregation was most likely caused by the screening effect of the low molecular weight salts, leading to increased hydrophobicity. On the other hand, the effect of raising the temperature above the PNIPAM phase transition on the structural density was similar to the situation observed in water (Figure 5). The structural density was not affected by the charge screening effect of salts and showed similar trend as in water.

Electron microscopy was used to gain further insight into the temperature-dependent behavior of the TRC(4.2, 62)/DNA complexes formed at $\varphi = 1.2$ and 2.0 (Figure 9). The electron micrographs confirm poor condensing ability of TRC(4.2, 62) at $\varphi = 1.2$ with no observable particles. The absence of particles was probably caused by the incomplete condensation of DNA, low structural density, and negative surface charge, all factors contributing to poor adhesion and staining of the formed structures. Well-stained particles were observed for the positively charged complexes formed at the molar mixing ratio of 2. The samples deposited at 37 °C generally exhibited better staining, and signs of aggregation were observed for complexes at $\varphi = 2$, confirming the light scattering data. Although well-stained particles were observed also for the complexes formed at $\varphi = 1.2$, the presence of fibrous structures indicated the presence of poorly condensed DNA—a fact that may help to explain the increase in M_w with increasing PNIPAM content at $\varphi = 1.2$.

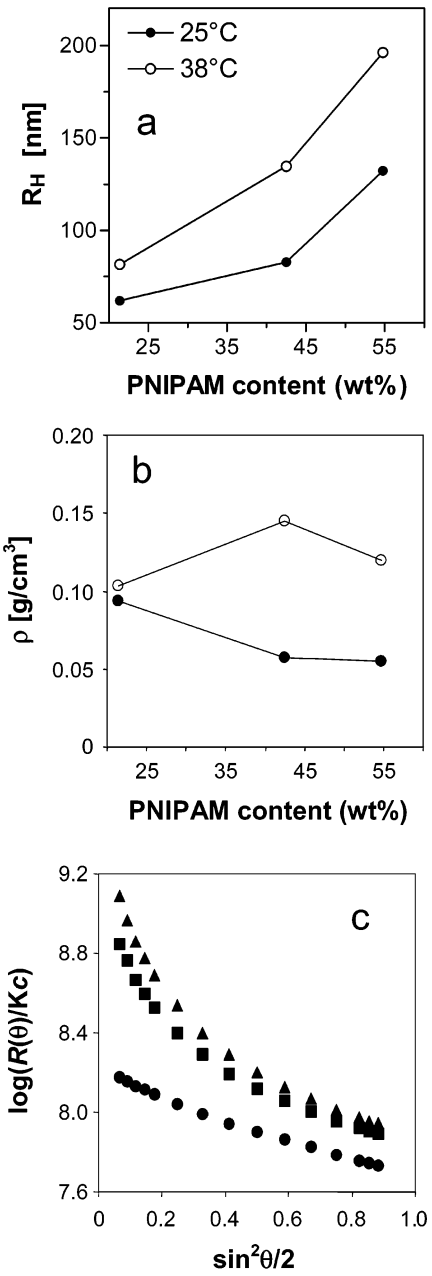

Figure 8. Effect of temperature on molecular parameters of TRC(12.4, *y*)/DNA complexes formed at $\varphi = 1.2$ in 10 mM HEPES buffer pH 7.4. The DNA complexes were formed using TRC copolymers containing PNIPAM with molecular weight 12 400, and (a) hydrodynamic radius (R_H) and (b) structural density (ρ) were determined at 25 °C (●) and 38 °C (○). A Guinier plot of scattering curves for TRC(12.4, y)/DNA complexes in 10 mM HEPES measured at 38 °C (c): TRC(12.4, 55) (triangles), TRC(12.4, 42) (squares), TRC(12.4, 21) (circles).

We have further tested whether the temperature-induced changes of structural density of the complexes were associated with changes of DNA conformation. We acquired circular dichroism spectra of the complexes below and above the PNIPAM phase transition (data not shown). Only small, PNIPAM-independent changes

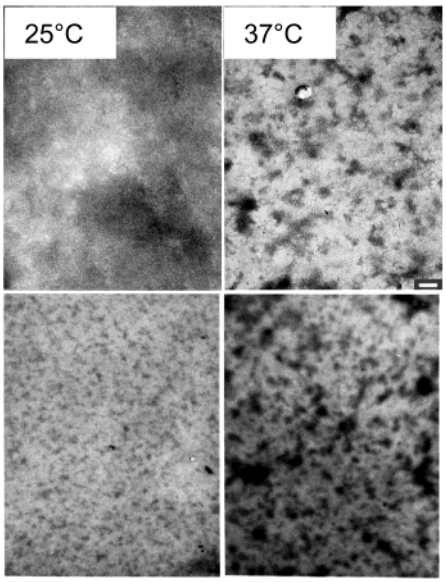

Figure 9. Electron microscopy of TRC(4.2, 62)/DNA complexes. The morphology was evaluated for TRC(4.2, 62)/DNA complexes formed in water using $\varphi = 1.2$ at 25 °C (top left panel) and 37 °C (top right panel) (magnification 25 000) and TRC(4.2, 62)/DNA complexes formed using $\varphi = 2$ at 25 °C (bottom left panel) and 37 °C (bottom right panel) (magnification 15 000) (bar 200 nm).

of the CD spectra of the complexes were observed upon increasing the temperature from 25 to 38 °C. The major changes in the CD spectra resulted from the presence of PNIPAM. Increasing the content of PNIPAM in the copolymers resulted in the disappearance of a positive CD band at 220 nm observed for PLL/DNA and appearance of two negative CD bands at 210 and 225 nm.

Release of DNA from the polyelectrolyte complexes is an important step in the gene delivery process. It is likely that at least part of the DNA at a time must be liberated from the complexes to be available for transcription in the cell nucleus. In addition, not only the release per se but also its timing, kinetics, and location are crucial factors for efficient gene delivery.[35] Polyelectrolyte exchange reactions are the most likely mechanism of such DNA release. Better understanding of the exchange reactions is therefore important for the optimization of the design of efficient gene delivery vectors.[36−39]

Herein, we discuss preliminary data on selected aspects of polyelectrolyte exchange reactions of PLL/DNA and TRC(4.2, 62)/DNA complexes with heparin. The exchange reactions were studied at 25 °C, and effects of the PNIPAM presence, incubation temperature, molar mixing ratio, and the time between the formation of the complexes and addition of heparin ("age" of complexes) were examined (Figure 10a). The complexes were subjected to three temperature/time regimes as described in the Experimental Section. Irrespective of the used regime, more DNA was released from the complexes containing PNIPAM than from the PLL/DNA complexes. The release of DNA from the complexes became more difficult with aging of both PLL/DNA and TRC/DNA complexes. Except for a brief note in a paper by Cherng et al.,[40] the effect of aging on the exchange reactions, as documented in Figure 10a, was to our knowledge not reported previously. Increased temperature clearly accelerated the processes leading to increased resistance against exchange reactions in both PLL- and TRC(4.2, 62)-based complexes, although

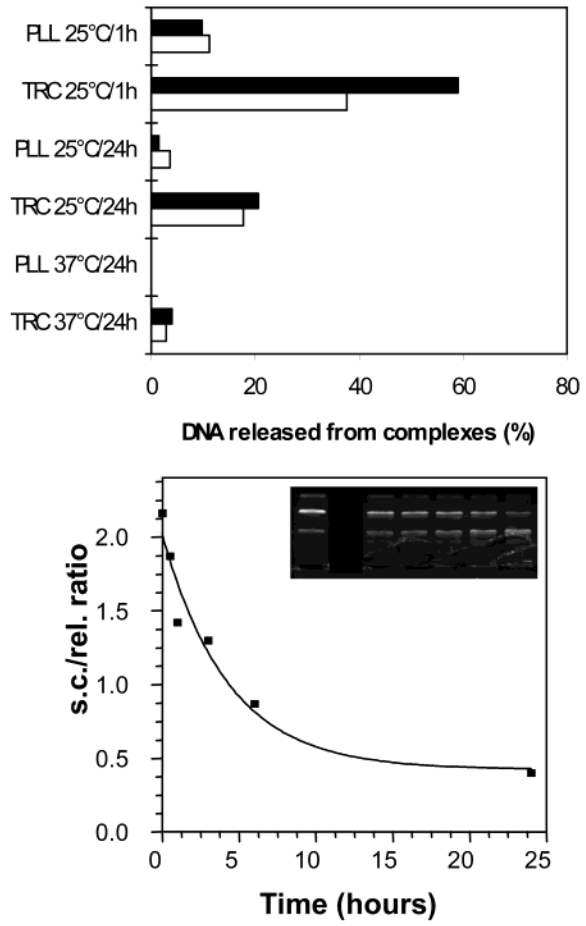

Figure 10. Polyelectrolyte exchange reactions of PLL/DNA and TRC(4.2, 62)/DNA complexes with heparin. The exchange reactions were studied by observing heparin-mediated release of free DNA from its complexes by agarose gel electrophoresis. (a) Complexes of plasmid DNA with TRC(4.2, 62) and PLL ($M_w = 87.6 \times 10^3$) were prepared 1 or 24 h before addition of heparin at $\varphi = 1.2$ (■) and 2 (□) and incubated at 25 or 37 °C. Heparin was then added, and the mixtures were incubated for an additional 2 h at 25 °C, and the total amount of DNA released from the complexes was quantified by electrophoresis. (b) Complexes of DNA with PLL ($M_w = 19.6 \times 10^3$) formed at $\varphi = 2$ were prepared 0.5−1−2.5−5−24 h before addition of heparin and analyzed by agarose gel electrophoresis (inset). The ratio between supercoiled and relaxed forms of DNA was calculated for each time point.

more distinctly in the case of TRC/DNA complexes. It should be however noted that the PLL/DNA complexes are relatively stable under the chosen conditions as documented by only a small amount of released DNA. Despite a very low amount of free DNA entering the gel, high fluorescent intensity (about 50% of the total DNA fluorescence intensity) was observed for PLL/DNA complexes in the loading well. The structural reasons of the fluorescence present in the loading well of the gel for PLL/DNA complexes are still under investigation.

A closer look at the data on polyelectrolyte exchange reactions revealed also surprising changes in DNA topology. A typical preparation of plasmid DNA contains the majority of supercoiled (sc) and minority of relaxed (rel) form. The DNA that was released from the complexes exhibited decreased ratio between supercoiled and relaxed forms of DNA with increasing time and temperature. To allow for more efficient release of DNA from the complexes, we prepared the complexes with PLL of lower molecular weight ($M_w = 19.6 \times 10^3$) and

studied the influence of the aging of the PLL/DNA complexes on the ratio between supercoiled and relaxed form in the DNA released from the complexes by heparin (Figure 10b). The DNA recovery from the complexes was nearly 70% and was almost constant at all the time points studied. The figure shows that when the complexes were incubated for longer times before the heparin addition the released DNA was found predominantly in the relaxed form. Because the amount of the released DNA was almost constant at each observed time point, the data suggest a conversion of the two forms rather than just preferential release of the relaxed form. In addition, in the latest time point in Figure 10b the amount of relaxed form of DNA is clearly higher than the amount in the starting DNA. Such a tendency of DNA in the complexes with polycations to be preferentially released in relaxed form was reported previously, but the time factor in the process was not recognized and no explanation was provided.[5,41] This phenomenon may have important consequences for the gene delivery because of the differential properties of the two forms of DNA (i.e., resistance against enzymatic degradation or transfection activity). The reasons, mechanisms, and consequences for the biological activity of the observed phenomenon will be further investigated.

Conclusions

In this study, the properties of polyelectrolyte complexes of DNA and thermoresponsive graft copolymers were investigated. We have demonstrated that the presence of PNIPAM in the structure of the complexes provides them with a temperature responsiveness that was manifested by significant differences of physicochemical properties below and above the phase transition temperature of PNIPAM. The most obvious differences were observed in structural density and surface charge of the complexes. This study demonstrates the potential use for temperature-responsive polymers in gene delivery and expands already wide use of these polymers in other biomedical applications. We anticipate that the changes in physicochemical properties of the complexes described in this study can be translated into modulation of biological activity. As such, these complexes can serve as a platform for further development of "smart" gene delivery vectors capable of changing their properties in a specific stimulus-dependent manner and contribute to further improvement of synthetic gene delivery vectors.

Acknowledgment. We thank Len Seymour and Karel Ulbrich for their encouragement and support, Simon Briggs for acquiring CD spectra, and Matthew Reed for technical assistance. Support of the Grant Agency of the Academy of Sciences of the Czech Republic (Grant A1050101), European Union (Grant QLK6CT200000280), and BBSRC is gratefully acknowledged.

References and Notes

(1) Wiethoff, C. M.; Middaugh, C. R. *J. Pharm. Sci.* **2003**, *92*, 203−217.
(2) Merdan, T.; Kopecek, J.; Kissel, T. *Adv. Drug Deliv. Rev.* **2002**, *54*, 715−758.
(3) Zuber, G.; Dauty, E.; Nothisen, M.; Belguise, P.; Behr, J. P. *Adv. Drug Deliv. Rev.* **2001**, *52*, 245−253.
(4) Oupicky, D.; Diwadkar, V. *Curr. Opin. Mol. Ther.*, in press.
(5) Oupicky, D.; Parker, A. L.; Seymour, L. W. *J. Am. Chem. Soc.* **2002**, *124*, 8−9.
(6) McKenzie, D. L.; Smiley, E.; Kwok, K. Y.; Rice, K. G. *Bioconjug. Chem.* **2000**, *11*, 901−909.
(7) Oupicky, D.; Carlisle, R. C.; Seymour, L. W. *Gene Ther.* **2001**, *8*, 713−724.
(8) Kakizawa, Y.; Harada, A.; Kataoka, K. *J. Am. Chem. Soc.* **1999**, *121*, 11247−11248.
(9) Kakizawa, Y.; Harada, A.; Kataoka, K. *Biomacromolecules* **2001**, *2*, 491−497.
(10) Balakirev, M.; Schoehn, G.; Chroboczek, J. *Chem. Biol.* **2000**, *7*, 813−819.
(11) Park, Y.; Kwok, K. Y.; Boukarim, C.; Rice, K. G. *Bioconjug. Chem.* **2002**, *13*, 232−239.
(12) Lynn, D. M.; Langer, R. *J. Am. Chem. Soc.* **2000**, *122*, 10761−10768.
(13) Boussif, O.; Lezoualch, F.; Zanta, M. A.; Mergny, M. D.; Scherman, D.; Demeneix, B.; Behr, J. P. *Proc. Natl. Acad. Sci. U.S.A.* **1995**, *92*, 7297−7301.
(14) Midoux, P.; Monsigny, M. *Bioconjug. Chem.* **1999**, *10*, 406−411.
(15) Putnam, D.; Gentry, C. A.; Pack, D. W.; Langer, R. *Proc. Natl. Acad. Sci. U.S.A.* **2001**, *98*, 1200−1205.
(16) Bromberg, L.; Levin, G. *Macromol. Rapid Commun.* **1998**, *19*, 79−82.
(17) Hinrichs, W. L. J.; Schuurmans-Nieuwenbroek, N. M. E.; van de Wetering, P.; Hennink, W. E. *J. Controlled Release* **1999**, *60*, 249−259.
(18) Kurisawa, M.; Yokoyama, M.; Okano, T. *J. Controlled Release* **2000**, *69*, 127−137.
(19) Kurisawa, M.; Yokoyama, M.; Okano, T. *J. Controlled Release* **2000**, *68*, 1−8.
(20) McCormick, C. L. *Stimuli-Responsive Water Soluble and Amphiphilic Polymers*; American Chemical Society: Washington, DC, 2001; Vol. 780.
(21) Watanabe, M.; Akahoshi, T.; Tabata, Y.; Nakayama, D. *J. Am. Chem. Soc.* **1998**, *120*, 5577−5578.
(22) Qiu, Y.; Park, K. *Adv. Drug Deliv. Rev.* **2001**, *53*, 321−339.
(23) Stayton, P. S.; Shimoboji, T.; Long, C.; Chilkoti, A.; Chen, G. H.; Harris, J. M.; Hoffman, A. S. *Nature (London)* **1995**, *378*, 472−474.
(24) Konak, C.; Oupicky, D.; Chytry, V.; Ulbrich, K.; Helmstedt, M. *Macromolecules* **2000**, *33*, 5318−5320.
(25) Dautzenberg, H.; Rother, G. *Makromol Chem., Macromol. Symp.* **1992**, *61*, 94−113.
(26) Dautzenberg, H.; Rother, G. *J. Polym. Sci., Polym. Phys.* **1988**, *26*, 353−366.
(27) Dautzenberg, H.; Gao, Y. B.; Hahn, M. *Langmuir* **2000**, *16*, 9070−9081.
(28) Dautzenberg, H.; Zintchenko, A.; Konak, C.; Reschel, T.; Subr, V.; Ulbrich, K. *Langmuir* **2001**, *17*, 3096−3102.
(29) Bronich, T. K.; Nguyen, H. K.; Eisenberg, A.; Kabanov, A. V. *J. Am. Chem. Soc.* **2000**, *122*, 8339−8343.
(30) Konak, C.; Reschel, T.; Oupicky, D.; Ulbrich, K. *Langmuir* **2002**, *18*, 8217−8222.
(31) Oupicky, D.; Konak, C.; Ulbrich, K. *J. Biomater. Sci., Polym. Ed.* **1999**, *10*, 573−590.
(32) Dautzenberg, H. *Macromolecules* **1997**, *30*, 7810−7815.
(33) Kriz, J.; Dautzenberg, H. *J. Phys. Chem. A* **2001**, *105*, 3846−3854.
(34) Kriz, J.; Dybal, J.; Dautzenberg, H. *J. Phys. Chem. A* **2001**, *105*, 7486−7493.
(35) Varga, C. M.; Hong, K.; Lauffenburger, D. A. *Mol. Ther.* **2001**, *4*, 438−446.
(36) Bakeev, K. N.; Izumrudov, V. A.; Kuchanov, S. I.; Zezin, A. B.; Kabanov, V. A. *Macromolecules* **1992**, *25*, 4249−4254.
(37) Izumrudov, V. A.; Bronich, T. K.; Saburova, O. S.; Zezin, A. B.; Kabanov, V. A. *Macromol. Chem., Rapid Commun.* **1988**, *9*, 7−12.
(38) Izumrudov, V. A.; Ortiz, H. O.; Zezin, A. B.; Kabanov, V. A. *Macromol. Chem. Phys.* **1998**, *199*, 1057−1062.
(39) Izumrudov, V. A.; Chaubet, F.; Clairbois, A. S.; Jozefonvicz, J. *Macromol. Chem. Phys.* **1999**, *200*, 1753−1763.
(40) Cherng, J.-Y.; Schuurmans-Nieuwenbroek, N. M. E.; Jiskoot, W.; Talsma, H.; Zuidam, N. J.; Hennink, W. E.; Crommelin, D. J. A. *J. Controlled Release* **1999**, *60*, 343−353.
(41) Oupicky, D.; Ogris, M.; Howard, K. A.; Dash, P. R.; Ulbrich, K.; Seymour, L. W. *Mol. Ther.* **2002**, *5*, 463−472.

MA034039A